Paper accepted for presentation at 2009 IEEE Bucharest Power Tech Conference, June 28th - July 2nd, Bucharest, Romania

Bifurcations and loadability issues in power systems

Héctor A. Pulgar-Painemal, Peter W. Sauer.

***Abstract*—This paper deals with bifurcations and loadability issues in power systems. A single machine system with dynamic state space represented by a set of differential algebraic equations is considered. It is emphasized that this small system can give a first step in understanding the issues discussed in this paper. Using system loading as a bifurcation parameter and considering two methodologies for calculating system equilibrium points—specification of a fixed terminal voltage and a voltage-controller reference—the incidence of voltage imposed by the machine in the system stability is studied. The results of this paper reveal that careful attention must be paid to all methodologies for calculating equilibrium points, as some may obscure likely solutions in the state space. In addition, a proper adjustment of a machine voltage-controller reference can be exploited to provide relief to a system when it is operating close to collapse.**

***Index Terms*—Voltage Stability, Voltage Collapse, Dynamic Systems, Bifurcations**

I. Introduction

A power system aims to provide power to loads in a secure and reliable way. A power system has to withstand the effects of endogenous and extraneous contingencies as well as natural growth in the system load. The last stresses the system and causes contingency effects to be more severe. The most recent major blackout in North America is an example of contingencies having a devastating effect due to excessive loading [1]. Loading is a major issue generally related to low voltage and voltage collapse.

Typically, the study of this issue is done by considering loading as a parameter in bifurcation studies. A Hopf bifurcation (HB) point in state space can be considered as a boundary of a secure operation. If that point is passed the system becomes dynamically unstable. If the system is operated far from an HB point, a stability margin can be obtained. However, due to power system economics and markets, this margin cannot be easily found. Nowadays, power systems are highly loaded during peak hours, making the study of nonlinear bifurcations and dynamic stability extremely important. When an HB point is exceeded, new stationary equilibrium points, periodic orbits, and chaotic behavior may occur. In [2], catastrophic bifurcations, such as the saddle-node bifurcation (SNB), subcritical HB and chaotic blue-sky bifurcation, have been studied in a single machine system. Similarly, using three- and nine-bus test systems, bifurcations and chaotic behavior have been observed while the effects of flexible ac transmission systems ($FACTS$) devices in the elimination of bifurcations have been explored [3]. In addition, state feedback has been proposed to control bifurcation and chaotic behavior [4]. However, a classical model for synchronous machine was used in those studies, i.e., a classical swing-equation model. In this article, a two-axis model is used [5].

Many studies have been done on the effects of loads, as loading is a prime factor in instabilities. Static loads, e.g., constant-power, -current and -impedance; and dynamic loads, e.g., induction machines of various model orders; have been addressed [6]–[9]. In respect to the static-load models, it has been demonstrated that the constant-power-load model causes the lowest dynamic loading margin [7] and has a considerable impact on the SNB point [8], [9]. However, the incidence of voltage imposed by machines in system stability has not been properly studied.

A single machine system with dynamic state space represented by a set of differential algebraic equations is considered. Two methodologies—specification of a fixed terminal voltage and a voltage-controller reference—for calculating the system equilibrium points are considered in order to show the importance of the voltage imposed by the machine in the system stability. It is emphasized that this small system can give a first step in understanding the incidence of machine voltages. Basically, it is shown that by adjusting the voltage-controller reference, an SNB point in the state space can be shifted, creating a whole stable neighborhood around the nose of the power-voltage (PV) curve. In addition, new stationary equilibrium points are discovered. Depending on the machine voltage, several limit points may appear. The results of this work reveal that careful attention must be paid to all methodologies for calculating equilibrium points, as some may obscure likely solutions in the state space. In addition, a proper adjustment of a machine voltage-controller reference can be exploited to provide relief to a system when it is operating close to collapse.

This paper is structured as follows. In Section II a brief description of nonlinear phenomena is described. In Section III the dynamic model of the system under study is presented. In Section IV two cases are presented to show the importance of the voltages imposed by the machines on system stability. Finally, in Section V conclusions are presented.

II. Basic nonlinear phenomena

Nonlinearity and parameter dependence are characteristics inherent in power systems. These are autonomous and typically described by a set of differential algebraic equations. Branching or bifurcation diagrams can be used to understand system behavior. Basically they describe the trajectory of either stationary equilibrium points or periodic orbits in the state space when some parameters are varied, i.e., bifurcation parameters. The number of solutions and the system stability may change depending on the bifurcation parameter value and the branch that the system follows (Figure 1). The local

H. Pulgar-Painemal and P. Sauer are with the Department of Electrical and Computer Engineering, University of Illinois at Urbana-Champaign, IL, 61801 USA e-mail: hpulgar2@illinois.edu and psauer@illinois.edu.

978-1-4244-2235-7/09/$25.00 ©2009 IEEE

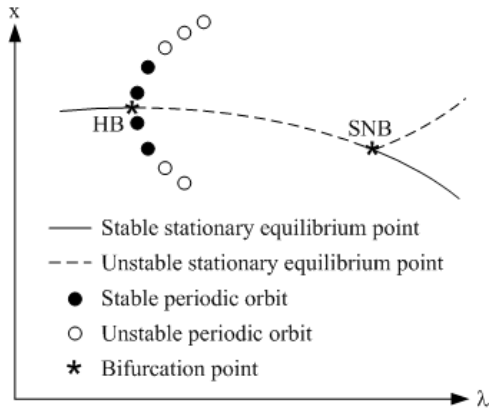

Fig. 1. Bifurcation diagram of an hypothetic state variable x in terms of the bifurcation parameter λ

stability of the system around a stationary equilibrium point depends on the location of the system eigenvalues. Definitions such as *stable node, unstable node, saddle, stable focus, unstable focus* and *center* are considered [10]. The stability of system periodic orbits can be determined using Floquet multipliers [11]. When a single pair of complex eigenvalues crosses the imaginary axis to the positive real side and no other eigenvalue has a nonnegative real part, then "there is a birth of limit cycles" [11]. This bifurcation defines new trajectories of periodic orbits. The crossing point is called a Hopf bifurcation point.

Saddle-node bifurcation points (SNB) and turning points are important for representing system behavior in state space. An SNB point is characterized by a zero eigenvalue and receives its name from the collision of a saddle and a node. Turning points, also known as limit points (LP), reflect change in the direction of state variable trajectories. For example, in the classical PV curve, the limit point corresponds to the nose of the curve. Note that an LP does not always coincide with an SNB point [11]. Moreover, when the system hits an SNB point, new stationary equilibrium points or periodic orbits can arise [2].

Power system analysis methods, thus, must be carefully designed due to complex system behavior as well as to the appearance of new trajectories in state space. Because all possible trajectories must be identified in order to avoid an unexpected system behavior, appropriate methods, models, and procedures to perform power system analysis are needed.

III. System Modeling

A. Dynamic Model

The dynamic behavior of a power system is represented by a set of differential algebraic equations (DAE) as

$$\dot{x} = f(x, y, \mu) \tag{1}$$
$$0 = g(x, y, \mu) \tag{2}$$

where x is a vector of the state variables, y is a vector of the algebraic variables, μ is a vector of the inputs and f and g are non-linear functions. The algebraic equations are derived from high order models where it is assumed that the machine-stator and electrical-network dynamics are extremely fast compared to the slow dynamics associated to the machine controllers. A zero order manifold is obtained to represent the fast variables, i.e., Equation (2). Based on the level of detail, several dynamic models, including the two-axis or the flux-decay model, may be used [5], [12].

Consider a single lossless synchronous machine connected to a load through a lossless transmission line (Figure 2). Assume that the machine is represented by a two-axis model [5] and that the transient reactance at both quadrature and direct axes are equal, i.e., $X'_d = X'_q$. Moreover, assume an IEEE Type 1 Exciter without saturation and a linear speed governor. Additionally, use an exponential model for the load, $P_L = P_o V_2^{pv}$ and $Q_L = Q_o V_2^{qv}$. Then the set of DAE is defined by

1) Differential equations:

$$T'_{do}\dot{E}'_q = -E'_q - (X_d - X'_d)I_d + Efd \tag{3}$$
$$T'_{qo}\dot{E}'_d = -E'_d + (X_q - X'_q)I_q \tag{4}$$
$$\dot{\delta} = \omega - \omega_s \tag{5}$$
$$\frac{2H}{\omega_s}\dot{\omega} = T_M - E'_d I_d - E'_q I_q \tag{6}$$
$$T_E\dot{E_{fd}} = -K_E E_{fd} + V_R \tag{7}$$
$$T_F\dot{R}_f = -R_f + \frac{K_F}{T_F}E_{fd} \tag{8}$$
$$\frac{T_A}{K_A}\dot{V_R} = -\frac{V_R}{K_A} + R_f - \frac{K_F}{T_F}E_{fd} + (V_{ref} - V_1) \tag{9}$$
$$T_{CH}\dot{T_M} = -T_M + P_{SV} \tag{10}$$
$$T_{SV}\dot{P_{SV}} = -P_{SV} + P_C - \frac{1}{R_D}\left(\frac{\omega}{\omega_s} - 1\right) \tag{11}$$

2) Algebraic equations:

$$P_o V_2^{pv} + jQ_o V_2^{qv} = V_2 e^{j\theta_2}(I_d - jI_q)e^{-j(\delta - \frac{\pi}{2})} \tag{12}$$
$$(E'_d + jE'_q) = j(X'_d + X_e)(I_d + jI_q) + V_2 e^{j(\frac{\pi}{2} + \theta_2 - \delta)} \tag{13}$$
$$V_1 e^{j\theta_1} = jX_e(I_d + jI_q)e^{j(\delta - \frac{\pi}{2})} + V_2 e^{j\theta_2} \tag{14}$$

Equations (12)–(14) can be manipulated to obtain the following set of real algebraic equations

$$0 = P_o V_2^{pv} + \frac{V_2}{X'_d + X_e}\left(E'_d \cos\theta'_2 + E'_q \sin\theta'_2\right) \tag{15}$$
$$0 = Q_o V_2^{qv} - \frac{V_2}{X'_d + X_e}\left(E'_q \cos\theta'_2 + E'_d \sin\theta'_2\right) \tag{16}$$
$$0 = -(X'_d + X_e)I_q - E'_d - V_2 \sin\theta'_2 \tag{17}$$
$$0 = (X'_d + X_e)I_d - E'_q + V_2 \cos\theta'_2 \tag{18}$$
$$0 = -V_1 \cos\theta'_1 + X_e I_d + V_2 \cos\theta'_2 \tag{19}$$
$$0 = -V_1 \sin\theta'_1 + X_e I_q + V_2 \sin\theta'_2 \tag{20}$$

where $\theta'_1 = \theta_1 - \delta$ and $\theta'_2 = \theta_2 - \delta$. Note that in this small system, state variable δ is not required, so that Equation (5) may be deleted. Thus,

$$x = [E'_q, E'_d, \omega, E_{fd}, R_f, V_R, T_M, P_{SV}]^T \tag{21}$$
$$y = [V_1, \theta'_1, V_2, \theta'_2, I_q, I_d]^T \tag{22}$$
$$\mu = [V_{ref}, P_C]^T \tag{23}$$

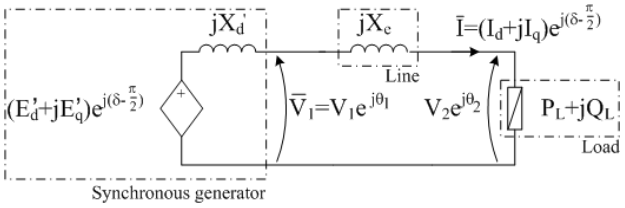

Fig. 2. Single-machine system

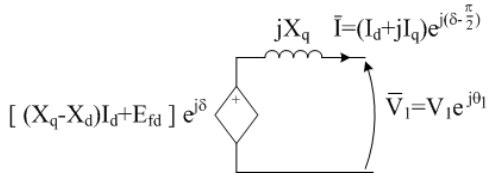

Fig. 3. Steady-state model of a synchronous machine

An important model to calculate equilibrium points or initial conditions is the steady-state machine model (Figure 3). Given the complex voltage and current at the terminal of the machine, δ and E_{fd} can be easily calculated [5]. The angle δ is typically known as the *angle behind the quadrature reactance*.

B. Equilibrium point calculation

In general, an equilibrium point is found by solving

$$f(x, y, \mu) = 0 \tag{24}$$
$$g(x, y, \mu) = 0 \tag{25}$$

Note that the voltage controller is modeled by Equations (7)–(9). A tracking control is considered such that the terminal voltage (V_1) follows a voltage reference (V_{ref}). However, for simplicity, it has been a common practice to specify a terminal voltage rather than a voltage-controller reference. Consequently, for every equilibrium point, V_{ref} has to be adjusted such that V_1 is kept at its specified value.

Specifying a terminal voltage rather than a voltage-controller reference is convenient because a conventional power-flow algorithm can be used to calculate voltages and injected currents at every bus. On the other hand, a generalized power-flow formulation must be used to calculate voltages and currents if V_{ref}, rather than the terminal voltage, is specified [13], [14]. Thus, the calculation of an equilibrium point is dependent on whether a specified V_{ref} or V_1 is assumed. Methodologies are presented for both cases.

Methodology A – Specify a fixed terminal voltage: This is the most common methodology used in power system analysis [8], [9], [15], [16]. Consider our single-machine system with a fixed terminal voltage, i.e., V_1 is constant. Then the steps to calculate the equilibrium point are the following:

- Using $\overline{V}_1$ as angle reference and given P_o and Q_o, run a power-flow algorithm to determine $\overline{V}_2$ and $\overline{I}$.
- Calculate δ using the steady-state model.
- Calculate I_d and I_q using $I_d + jI_q = \overline{I}e^{j(\frac{\pi}{2}-\delta)}$.
- Calculate E_{fd} using the steady-state model.
- Sequentially set Equations (3) to (11) to zero and calculate the state variables and the inputs, i.e., P_C and V_{ref}.

TABLE I
SYSTEM DATA

X_d	X_q	X'_d	X'_q	T'_{do}	T'_{qo}	H	R_D
2.2	1.76	0.2	0.2	8	1	3.5	0.05
K_E	T_E	K_F	T_F	K_A	T_A	T_{CH}	T_{SV}
1	0.7	0.03	1	200	0.04	0.05	0.1

In the absence of bifurcations there is a one-to-one correspondence between V_{ref} and V_1. However, in the presence of bifurcations, at a particular V_{ref} multiple solutions for $\overline{V}_1$ may exist. Therefore, the main drawback of this methodology is that for the same calculated V_{ref}, another voltage solution may exist which will define a different equilibrium point.

Methodology B – Specify V_{ref}: In this case the equilibrium point has to be found by simultaneously solving the set of nonlinear equations defined by Equations (24) and (25). Having a fixed V_{ref}, the terminal voltage may drop—depending on the machine parameters, network parameters and loading level. In order to avoid an excessive voltage drop, $V_{ref}(P_o)$ can be specified, i.e., V_{ref} in terms of loading level, P_o. The main advantage of this methodology is that all possible equilibrium points are considered because $\overline{V}_1$ is treated as a variable and not as a specified value.

C. Linearization

Linearize the DAE defined by Equations (1) and (2) at an equilibrium point to obtain

$$\Delta\dot{x} = A\Delta x + B\Delta y \tag{26}$$
$$0 = C\Delta x + D\Delta y \tag{27}$$

Using Kron's reduction, algebraic equations are eliminated:

$$\Delta\dot{x} = (A - BD^{-1}C)\Delta x = A_{sys}\Delta x \tag{28}$$

Eigenvalues of A_{sys} define the stability of the operating point. Use load P_o as a bifurcation parameter. Then, for every single value of P_o, calculate the eigenvalues of A_{sys} to determine the system stability.

IV. CASES

Two issues are addressed with the following cases. Firstly, the structural stability of a system is highly dependent on the voltage imposed by the machine controllers. Secondly, when Methodology A is used to calculate the system equilibrium point, some regions of the state space are obscured. New operating points are discovered using the Methodology B. Machine parameters are presented in Table I. The transmission line has a series reactance of $X_e = 0.1[pu]$. Note that the secondary frequency control of the governor is not explicitly modeled, so P_C is adjusted at every loading level to maintain synchronous speed, i.e., $\omega = \omega_s$. A constant-power load model is considered, i.e., $pv = 0$ and $qv = 0$. Finally, for Methodology B, a Newton-Raphson routine is used to solve the set of nonlinear equations.

A. Effect of machine voltage on system stability

System stability has been studied considering the load as a bifurcation parameter under different load models without taking into consideration the importance of the voltage imposed by the machine controllers. It has been observed that the eigenvalue movements follow a well known pattern [5], [8], [9]. Assume that at a specified loading level the system is stable, i.e., all eigenvalues are on the left half plane. As the loading is increased, a complex pair of eigenvalues, generally associated with the voltage controller variables, moves to the right and at a point crosses the imaginary axis defining the Hopf bifurcation point. If the load is further increased, these complex eigenvalues, on the right half plane, will coalesce on the real line and then split into two real eigenvalues moving in opposite directions. The one moving to the right will keep increasing until it comes back through infinity to the left half plane. At infinity, the Jacobian associated with the algebraic variables, i.e., D, becomes singular. This is known as a *singularity-induced bifurcation point*. The other real eigenvalue, still on the right half plane, drifts to the origin as the load is increased. When it reaches zero the full Jacobian of the DAE becomes singular. This is an SNB point. In some cases the SNB point coincides with the LP or maximum power point, depending on the voltage imposed by the controllers as well as the load model. In Figure 4, eigenvalue movement is depicted when V_{ref} is constant and equal to 1.005.

In order to show the effects of machine voltage on system stability, both Methodologies A and B are considered. While a fixed machine terminal voltage is assumed in Methodology A, a fixed V_{ref} is considered in Methodology B. The PV curves obtained at bus 2 using both methodologies are presented in Figure 5. A solid line represents a stable equilibrium point while a dashed line represents an unstable one. Unsurprisingly, the maximum transmitted power is reduced when the second methodology is used. Additionally, the HB point occurs at an earlier loading level. What is surprising is that the structural stability around the maximum power point is radically different. Assuming a fixed terminal voltage, the SNB point occurs before the LP. The LP is dynamically stable. On the other hand, assuming a fixed V_{ref}, the SNB point takes place in a small neighborhood around the LP which is likely to be unstable. Although not found using a Newton-Raphson routine, the solution at the SNB point is bounded by the solutions from the upper and lower side of the PV curve. The gap between the upper and lower solutions can be considered small enough (see Table II). From these results, as a proper adjustment of the voltage-controller reference can make a whole neighborhood around the LP stable, it is inferred that this phenomenon can be exploited to provide relief to a system operating close to collapse.

B. Bifurcations and maximal loadability

In the real world, most of the generating units are controlling voltages in specified buses. Generally, these controlled buses correspond to machine terminals. A desired terminal voltage is pursued by setting a reference in the machine voltage controller, i.e., V_{ref}. Therefore, specifying a machine terminal voltage, as in Methodology A, rather than a voltage-controller

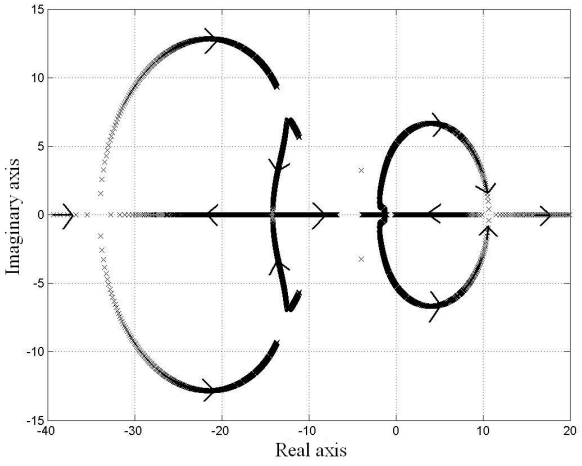

Fig. 4. Eigenvalues of A_{sys} at the upper side of the PV curve

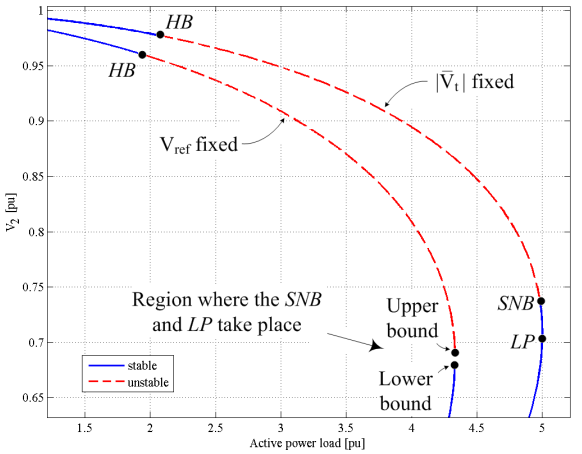

Fig. 5. Comparison between two strategies for voltage control

TABLE II
CLOSEST SOLUTIONS TO THE MAXIMUM POWER THROUGH THE UPPER AND LOWER SIDE OF THE PV CURVE

	Upper side	*Lower side*
E'_q	1.913	1.957
E'_d	0.580	0.566
$E_{fd} = V_R$	14.394	14.747
R_f	0.432	0.442
$T_M = P_{SV}$	4.330	4.330
I_d	6.240	6.395
I_q	0.372	0.363
V_1	0.933	0.931
θ'_1	-0.777	-0.756
V_2	0.693	0.676
θ'_2	-1.511	-1.514
V_{ref}	1.005	1.005
$\max \Re(\lambda_i)$	0.048	-0.046

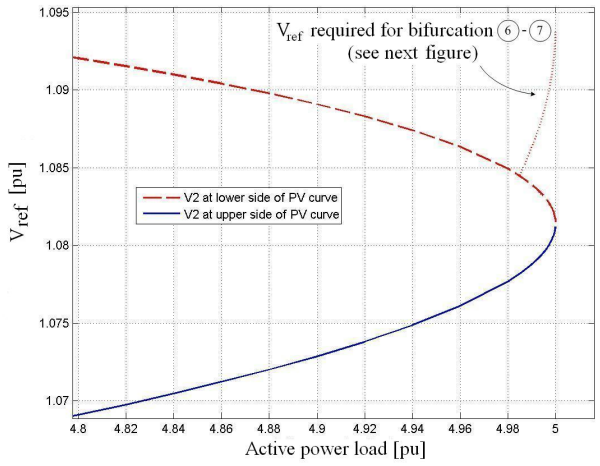

Fig. 6. $V_{ref}(P_o)$ for methodology A with $V_1 = 1$ $[pu]$

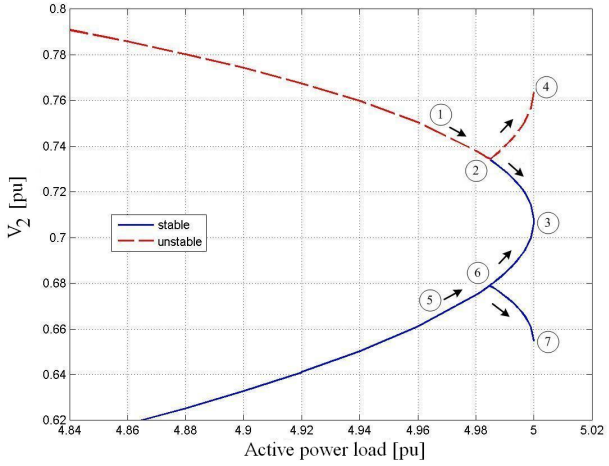

Fig. 7. PV curve using $V_{ref}(P_o)$

reference, as in Methodology B, is not realistic. Moreover, specifying a terminal voltage may obscure some likely operating points which show up when a voltage-controller reference is specified. In the following example, new equilibrium points are shown in a single-machine system. Methodology B is used. $V_{ref} = V_{ref}(P_o)$ is considered so that $V_1 = 1[pu]$.

First, the solution obtained in the previous subsection IV-A using Methodology A is a particular solution where V_{ref} was adjusted in order to keep $V_1 = 1[pu]$. $V_{ref}(P_o)$ is obtained. In Figure 6, V_{ref} is shown when the operating point belongs either to the upper or the lower side of the PV curve. A solid line corresponds to an operating point on the upper side of the PV curve while a dashed line correspond to an operating point on the lower side.

Now, use Methodology B with $V_{ref}(P_o)$ of Figure 6 to solve for the equilibrium points at different loading levels in the range of $P_o = 0$ to $P_o = 5[pu]$. From $P_o = 0$ to $P_o = 4.9848[pu]$ (SNB point) the same solution is found as when using Methodology A. However, after the SNB point, another solution arises with higher values for voltages V_1 and V_2. This bifurcation in the equilibrium point trajectory is shown in Figure 7. According to the eigenvalues of A_{sys}, the new solution that bifurcates upward on the PV curve is unstable. Thus, after the SNB point, the system can either take the trajectory ①→②→③, which is stable, or the trajectory ①→②→④, which is unstable. Both trajectories reach a maximum power point at $P_o = 5[pu]$. This example clearly shows that a solution which is unstable and undetectable using Methodology A may appear in the system. Moreover, it turns out that the point of maximum transfer is not unique.

Considering the quadratic characteristic of voltages, the solution that bifurcates upward has a second solution for V_2 by symmetry. This is obtained from

$$V_2 = +\sqrt{\frac{V_1^2 \pm \sqrt{V_1^4 - 4X_e^2P^2}}{2}} \qquad (29)$$

This new solution appears on the lower side of the PV curve which has a lower value for V_2 (trajectory ⑥→⑦ in Figure 7). This bifurcation also has a maximum power point at $P = 5[pu]$. Using the full set of DAE, it is verified that in fact this is effectively a trajectory of equilibrium points. However, these equilibrium points require an increase of V_{ref} (see dotted line in Figure 6) which is not allowed. Note that V_{ref} was already defined as the solid and dashed curve for the upper and lower side of the PV curve, respectively. Therefore, although both trajectories are stable, trajectory ⑤→⑥→③ is allowed and trajectory ⑤→⑥→⑦ is not. A summary of the solutions at the bifurcation points and at the maximum power points is shown in Table III.

TABLE III
SOLUTIONS AT BIFURCATIONS AND MAXIMUM POINTS

	$P\ 2$ (SNB)	$P\ 6$	$P\ 3$ (P_{max})	$P\ 4$ (P_{max})	$P\ 7$ (P_{max})
E'_q	2.0762	2.2334	2.0085	2.1537	2.3183
E'_d	0.6147	0.5688	0.6391	0.5929	0.5486
δ	0.7663	0.6967	0.0352	0.7328	0.6628
$E_{fd} = V_R$	15.6333	16.898	15.0797	16.2576	17.5729
R_f	0.4690	0.5069	0.4524	0.4877	0.5272
$T_M = P_{SV}$	4.9848	4.9848	5	5	5
I_d	6.7786	7.3323	6.5356	7.0520	7.6273
I_q	0.3940	0.3646	0.4097	0.3801	0.3517
V_1	1	1	1.0059	1	1.0059
θ'_1	-0.7663	-0.6967	-0.7993	-0.7328	-0.6628
V_2	0.7341	0.679	0.7635	0.7080	0.6548
θ'_2	-1.5127	-1.5211	-1.5082	-1.517	-1.5247
V_{ref}	1.0782	1.0845	1.0813	1.0813	1.0938
$\max \Re(\lambda_i)$	0	-0.2573	0.1351	-0.1263	-0.3701

V. CONCLUSIONS

A single machine system with dynamic state represented by a set of differential algebraic equations is considered. Using a two-axis dynamic model for the synchronous machine, two methodologies to calculate power system equilibrium points are presented. Methodology A considers a machine-controlled voltage as an input. This voltage is fixed at a specified value

and the voltage-controller reference has to be adjusted at every equilibrium point. Methodology B considers the voltage-controller reference as an input. If the reference is fixed, the controlled voltage may drop with the loading, depending on the machine and network parameters. If the reference is adjusted according to the load level, the voltage drop may be eliminated, thus keeping the desired voltage at the controlled bus. With these two methodologies and using a single machine test system, two important conclusions are obtained.

Firstly, it is shown that the system's structural stability strongly depends on the voltage imposed by the machine controllers. For our test system, using Methodology A, the SNB point occurs before the LP (nose of the PV curve). Thus the LP is dynamically stable. Using Methodology B with a fixed voltage-controller reference, the SNB point and LP are located at the same place in the state space. Thus, the LP is dynamically unstable. Secondly, when the voltage-controller reference is adjusted such that the machine terminal voltage is constant and nominal, it is observed that as soon as the SNB point is reached, new stationary equilibrium points arise. The trajectory of the new equilibrium points is dynamically unstable and the system bus voltages are increased. As a consequence, Methodology A, which assumes a fixed controlled voltage, is blinded before this bifurcation. In summary, if Methodology A is used in a power system analysis, careful attention must be paid to the analysis because this methodology obscures some solutions in the state space. In addition, it is inferred that a proper adjustment of the machine voltage-controller references can be exploited to provide relief to a system operating close to collapse.

In future work, this bifurcation analysis will be applied to a multi-machine system. In order to exploit the positive incidence of the machine voltage-controller reference in power system stability, further analysis needs to be performed due to the complexity of higher order systems.

REFERENCES

[1] G. Andersson, P. Donalek, R. Farmer, N. Hatziargyriou, I. Kamwa, P. Kundur, N. Martins, J. Paserba, P. Pourbeik, J. Sanchez-Gasca, R. Schulz, A. Stankovic, C. Taylor, V. Vittal, "Causes of the 2003 major grid blackouts in north america and europe, and recommended means to improve system dynamic performance," *IEEE Transactions on Power Systems*, vol. 20, no. 4, pp. 1922–1928, 2008.

[2] H.O. Wang, E.H. Abed, A.M.A. Hamdan, "Bifurcations, chaos and crises in voltage collapse of a model power system," *IEEE Transactions on Circuits and Systems - I: Fundamental Theory and Applications*, vol. 41, no. 3, pp. 294–302, 1994.

[3] K.N. Srivastava, S.C. Srivastava, "Elimination of dynamic bifurcation and chaos in power systems using FACTS devices," *IEEE Transactions on Circuits and Systems - I: Fundamental Theory and Applications*, vol. 45, no. 1, pp. 72–78, 1998.

[4] A.M. Harb, N. Abdel-Jabbar, "Controlling hopf bifurcation and chaos in a small power system," *Chaos, Solutions and Fractals*, vol. 18, pp. 1055–1063, 2003.

[5] P. W. Sauer and M. A. Pai, *Power systems dynamics and stability*. Prentice Hall, Upper Saddle River, NJ, 1998.

[6] W.D. Rosenhart, C.A. Cañizares, "Bifurcation analysis of various power system models," *Electric Power and Energy Systems*, vol. 21, pp. 171–182, 1999.

[7] N. Mithulananthan, C.A. Canizares, "Hopf bifurcations and critical mode damping of power systems for different static load models," *IEEE Power Engineering Society General Meeting*, vol. 2, pp. 1877–1882, 2004.

[8] C. Rajagopalan, B.C. Lesieutre, P.W. Sauer, M.A. Pai, "Dynamic aspects of voltage/power characteristics," *IEEE Transactions on Power Systems*, vol. 7, no. 3, pp. 990–1000, 1992.

[9] P.W. Sauer, B.C. Lesieutre, M.A. Pai, "Maximum loadability and voltage stability in power systems," *International Journal of Electrical Power and Energy System*, vol. 15, no. 3, pp. 145–154, 1993.

[10] H.K. Khalil, *Nonlinear Analysis*. Prentice-Hall, third ed., 2002.

[11] R. Seydel, *Practical bifurcation and stability analysis: From equilibrium to chaos*. Springer-Verlag, second ed., 1994.

[12] P. Kundur, *Power system stability and control*. McGraw-Hill, 1994.

[13] Z. Feng, V. Ajjarapu, B. Long, "Identification of voltage collapse through direct equilibrium tracing," *IEEE Transacctions on Power Systems*, vol. 15, no. 1, pp. 342–349, 2000.

[14] R. H. Yeu, P. W. Sauer, "Post-contingency equilibrium analysis techniques for power systems," *Proceeding of the 37th Annual North American Power Symposium*, pp. 429–433, 2005.

[15] C.A. Cañizares, "On bifurcations, voltage collapse and load modeling," *IEEE Transactions on Power Systems*, vol. 10, no. 1, pp. 512–522, 1995.

[16] A.A. Perleberg, C.A. Cañizares, A. Silveira e Silva, "Multiparameter bifurcation analysis of the south brazilean power system," *IEEE Transactions on Power Systems*, vol. 18, no. 2, pp. 737–746, 2003.